Density Peaking in the JFT-2M Tokamak Plasma with Counter Neutral-Beam Injection

K. Ida, S.-I. Itoh, K. Itoh, and S. Hidekuma
National Institute for Fusion Science, Nagoya, 464-01, Japan

Y. Miura, H. Kawashima, M. Mori, T. Matsuda, N. Suzuki, H. Tamai, T. Yamauchi, and JFT-2M Group
Japan Atomic Energy Research Institute, Naka-machi, Naka-gun, Ibaraki, 311-01, Japan
(Received 5 June 1991; revised manuscript received 18 October 1991)

A significant particle pinch and reduction of the effective thermal diffusivity are observed after switching the neutral beam direction from coinjection to counterinjection in the JFT-2M tokamak. The particle pinch measured in the counterinjection phase shows good agreement with the prediction of the inward pinch model related to the electric fields.

PACS numbers: 52.25.Fi, 52.30.−q, 52.55.Fa

The improvement of core confinement has been found to be associated with peaked electron density in various tokamak discharges. Many approaches to produce the peaked electron-density profile have been found. Central fueling with pellet injection in Ohmic discharge has extended the linear Ohmic confinement regime to higher densities in Alcator-C [1]. Beam fueling in low-density operation produced a peaked density plasma with a significantly high temperature in TFTR [2]. A rapid drop of external gas flux at the plasma edge can also produce peaked density profiles as demonstrated by reducing the gas puff or neon puffing (IOC mode) in ASDEX [3,4], or as observed at the transition from the H mode to the L mode under helium beam injection (improved L mode) in JFT-2M [5]. Recently, counter neutral-beam-injection (ctr-NBI) heating has been found to produce peaked density profiles and enhance the energy confinement time τ_E in ASDEX [6,7]. The relation between the momentum confinement and energy confinement has been discussed by TFTR and JET [8,9]. However, the mechanism of density peaking with ctr-NBI has not been clarified yet, although ASDEX data show that electron density and temperature profiles are consistent with reduction of the η_i mode. The improvement of particle confinement with counterinjection was first observed in ISX-B [10], and it was suggested theoretically that plasma confinement improvement by counterinjection could be the result of the suppression of turbulent fluctuation with more negative values of the radial electric field [11]. However, no quantitative comparison between measurements and theories has been done. In this paper, we present the connection between particle pinch and radial electric field for the plasma with peaked density profile measured for counterinjected neutral-beam discharge in the JFT-2M tokamak. Quantitative comparison with the inward particle pinch model [12] is also presented.

JFT-2M is a tokamak with major radius $R=1.3$ m and minor radius $a=0.35$ m. It has two tangential neutral beams; one is parallel (coinjection) and the other is antiparallel (counterinjection) to the plasma current. The profile of the radial electrical field was found to be affected by changing the direction of momentum input from coinjection to counterinjection [10,13]. We interchange the neutral beams from coinjection to counterinjection to study the response of the electric field and particle flux, keeping the absorbed power constant. These series of experiments were done under the conditions of a toroidal field B_t of 1.3 T, a plasma current I_p of 240 kA with limiter configuration, an elongation κ of 1.2, and NBI power of 0.5–0.6 MW at an injection energy of 32 keV. The profiles of the toroidal rotation velocity v_φ and ion temperature T_i are measured with multichannel charge-exchange spectroscopy (CXS) [14] every 16.6 ms using C VI ($\Delta n=8$-7) charge-exchange line emission. The time evolution of electron temperature at the center $T_e(0)$ is measured with a soft-x-ray pulse-height analyzer with 50-ms integration. Profiles of electron temperature and density n_e are obtained with a thirteen-channel Thomson scattering (TS) system. The line-averaged density $\bar{n}_e$ is given by a three-channel far-infrared (FIR) laser interferometer, and the total stored energy W_p is estimated from diamagnetic loops.

Figure 1 shows a typical example of the change in various plasma parameters, toroidal rotation velocity v_φ at $\rho=0.15$ (ρ being the averaged minor radius), line-averaged electron density $\bar{n}_e$ at $\rho=0.24$, total stored energy W_p, central electron temperature $T_e(0)$, central and volume-averaged ion temperatures $T_i(0)$ and $\langle T_i\rangle$, and peaking parameters of electron density and ion temperature profile, $n_e(0)/\langle n_e\rangle$, $T_i(0)/\langle T_i\rangle$, for a discharge where the neutral-beam direction is interchanged. The estimate of $n_e(0)/\langle n_e\rangle$ using the FIR laser is valid for the plasma with limiter configuration, where the edge electron density is (5–10)% of the central electron density and the density profiles measured with Thomson scattering are well fitted by a parabolic-shaped profile raised to some power as $n_e(\rho)=n_e(0)(1-\rho^2)^\alpha$ ($\alpha=1$-2). The peaking parameter of the electron-density profile $[n_e(0)/\langle n_e\rangle]$ can be determined from the value of α, which is estimated from the ratio of two line-averaged densities measured at $\rho=0.24$ and $\rho=0.6$. The co-NBI is activated from 550 to 750 ms with an absorbed power $P_{\rm abs}$ of 0.49 MW, and ctr-NBI is on from 750 to 950 ms with $P_{\rm abs}=0.56$ MW. The toroidal rotation velocity v_φ at $\rho=0.15$ changes within 30 ms after the onset of counterinjection, and the electric field, which is evaluated from the ion force bal-

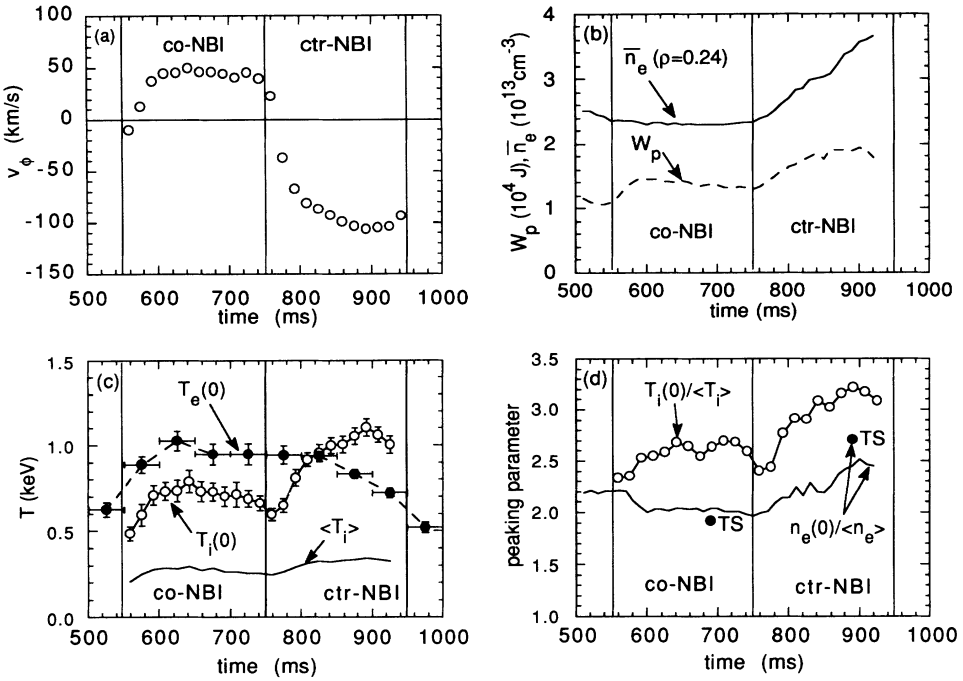

FIG. 1. Time evolution of (a) toroidal rotation velocity at $\rho=0.15$, (b) the line-averaged electron density and total stored energy, (c) central electron temperature, and central and volume-averaged ion temperatures, and (d) peaking parameters of the electron-density profile and ion temperature profile.

ance, changes in response to the change of rotation. Both $\bar{n}_e$ and W_p increase during the phase of counterinjection, and the energy confinement time is 18 ms for the co-NBI phase and 24 ms for the ctr-NBI phase. The total stored energy W_p saturates at $t=850$ ms and starts to decrease after $t=900$ ms. The saturation and decrease of the total stored energy at later times in the ctr-NBI phase are correlated with the decrease of electron temperature as shown in Fig. 1(c). The central electron temperature remains constant for 100 ms after ctr-NBI is initiated until impurities accumulate at the plasma center and the radiated power at the plasma center becomes comparable to the input power. On the other hand, the central ion temperature starts to increase as the plasma rotation increases its velocity in the opposite direction, and becomes higher than the electron temperature 100 ms after the ctr-NBI is turned on. This fact shows the significant improvement of heat transport during ctr-NBI. The $n_e(0)/\langle n_e\rangle$ values derived from the FIR laser interferometer agree with the results from the electron-density profile measured with TS in an initial phase, and give a slightly lower estimation at a later time. The density profile becomes flatter in the coinjection phase compared to the Ohmic phase, and shows peaking in the counterinjection phase. The peaking parameter of the ion temperature also shows peaking of the ion-temperature profile in the ctr-NBI phase.

The radial electric-field ($\partial\Phi/\partial r$) profile is given by the momentum balance equation [15]:

$$ev_\varphi B_\theta = -T_i\left(\frac{\partial \ln p_i}{\partial r} - (\beta_1, g_{2,i})\frac{\partial \ln T_i}{\partial r} + \frac{e}{T_i}\frac{\partial \Phi}{\partial r}\right), \quad (1)$$

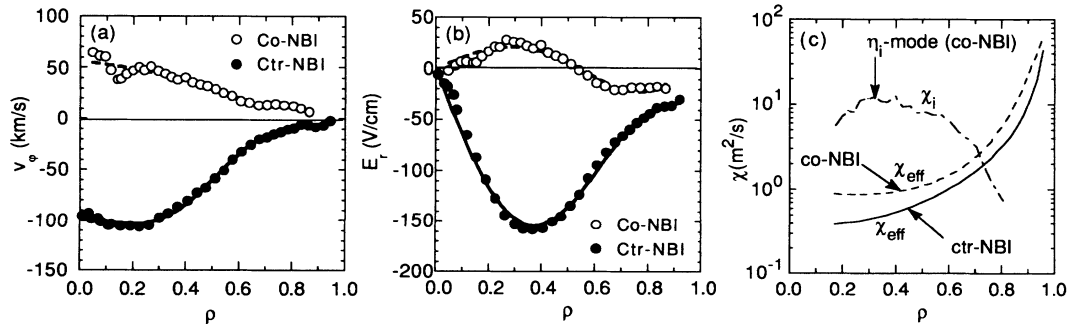

FIG. 2. Radial profiles of (a) toroidal rotation velocity, (b) radial electric field, and (c) effective thermal diffusivity in co-NBI phase ($t=690$ ms) and in ctr-NBI phase ($t=890$ ms).

where $\beta_1, g_{2,i}$ are numerical coefficients depending on the collisionality regime. Here we assume that carbon ions rotate as fast as bulk ions, $v_\varphi(C^{6+}) = v_\varphi(\text{bulk})$, which is a valid assumption at least when the toroidal rotation velocity is large enough (as shown in the ctr-NBI phase) to neglect the pressure gradient term in Eq. (1). The electron-density gradient is assumed to be as large as that for ions, $\partial n_e/\partial r = \partial n_i/\partial r$, since the profile of Z_{eff} contributed by C^{6+} is relatively flat. The profiles of toroidal rotation velocity, radial electric field, and thermal diffusivity at 690 and 890 ms are summarized in Fig. 2 for the discharge of Fig. 1.

An improvement of energy confinement with ctr-NBI compared to co-NBI is clear from Fig. 1, since the ion temperature and electron density increased with similar input powers. The energy flow is obtained from beam power deposition and energy transfer from, or to, electrons. The energy exchange between ions and electrons is reversed in the counterinjection phase. In order to avoid the error of the energy exchange between ions and electrons, we introduce an effective thermal conductivity defined by $q_{\text{cond}}/(n_e \partial T_e/\partial r + n_i \partial T_i/\partial r)$ as a measure of improvement in energy confinement. The effective conductivity is reduced in the ctr-NBI phase by a factor of 3, although the reduction of thermal diffusivity near the plasma edge is (30–50)% as shown in Fig. 2(c). The inward heat convection due to inward particle pinch is much smaller than the conduction. The majority of the change in χ_{eff} is due to the conductive part, not the convective part.

We evaluate the ion diffusivity χ_i predicted by the η_i mode theory [16,17] to check its validity. The η_i values are given by the ratio of ion temperature gradient to ion density gradient. They are evaluated at $t = 690$ ms in the coinjection and $t = 890$ ms in counterinjection phases from measured $T_i(r)$ and $n_e(r)$, assuming $\partial n_e/\partial r = \partial n_i/\partial r$. To evaluate the η_i value near the plasma center, both ion and electron temperature profiles are fitted with a polynomial function $[f(\rho) = c_0 + c_1\rho^2 + c_2\rho^4 + c_3\rho^6 + c_4\rho^8]$ with the boundary conditions of $\partial T_i/\partial r(0) = 0$ and $\partial n_i/\partial r(0) = 0$. The η_i values in the coinjection phase are above 1 everywhere in the plasma and increase towards plasma center. The η_i value at half of the plasma radius is $\eta_i(a/2) \sim 2$ and the central value is $\eta_i(0) \sim 10$ in the coinjection phase. In the counterinjection phase η_i values are almost constant in space and around unity. The predicted ion diffusivity χ_i by the η_i mode theory [17] for the co-NBI phase is of much higher value than the measured χ_{eff}, and the radial profiles are also quite different. In the case of ctr-NBI, the ion temperature gradient mode is predicted to disappear, since $\eta_i \sim 1$ everywhere in the plasma. The η_i mode theory shows no quantitative agreement with the measurements.

Next we discuss the particle flux in the co- and ctr-NBI phases. In the co-NBI phase, the density profile is in steady state, and there is no $\partial n_e/\partial t$. The outward particle flux during the co-NBI phase is balanced by particle deposition of co-NBI, while the particle flux in the counter phase is contributed from the particle deposition of ctr-NBI and $\partial n_e/\partial t$. The particle flux at $\rho < 0.6$ estimated from $\partial n_e/\partial t$ and the particle source is positive (outward) in the co-NBI phase, and it becomes negative (inward) for the ctr-NBI phase. The magnitude of the inward particle flux in the counter phase is comparable to that of the outward particle flux in the co-NBI phase. It is important to compare the measured density profiles with the prediction of the inward pinch model. According to the model, the particle flux is written as [12,18]

$$\Gamma = -D\left(\frac{\partial n}{\partial r} + \frac{\alpha \partial T}{\partial r}\frac{n}{T} - \frac{eE_r}{T}n + \frac{\omega B_t}{(m/r)T}n\right), \quad (2)$$

where D is a diffusion coefficient, α is a numerical coefficient of order unity, and ω and m/r denote the frequency and wave number of the mode for a drift-type microturbulence. Here the rigid rotation term due to E_r in the third and fourth terms in Eq. (2) cancel each other. Since there is almost no rigid rotation in the measured v_φ profile, i.e., $v_\varphi(a) \sim 0$, we can simply set $\omega = 0$ to neglect the fourth term. Using measured density and temperature gradients, and radial electric-field profiles, we can estimate the sign of particle flux without knowing the diffusion coefficients. This change of sign of particle flux shows qualitative agreement with the pinch model.

In order to make a quantitative comparison between measurements and model, we simulate the peaking of the electron-density profiles in the ctr-NBI phase with the diffusion coefficient profile obtained in the steady state of the co-NBI phase. In this simulation the electron-density profile measured with TS at $t = 690$ ms is taken as the initial profile, since the electron-density profile is in steady state in the co-NBI phase. Diffusion coefficients are derived from the particle source provided by NBI fast ions and the particle source from the plasma edge. The diffusion coefficient near the plasma edge is sensitive to the neutral density provided by the gas puff and recycling, while the diffusion coefficient at $\rho < 0.6$ is mainly determined by the amount of the source provided by NBI fast ions. Diffusion coefficients near the plasma center are 0.02 m^2/s, consistent with recent results of particle transport analysis in JET [19,20]. The simulated and measured electron-density profiles and time evolution of $\bar{n}_e$ are shown in Fig. 3. For both the radial profile and the magnitude of $\partial \bar{n}_e/\partial t$ there is good agreement. The simulated electron-density profiles are more peaked than the measured profiles as shown in Fig. 3(a). This is due to sawtooth-oscillations effects on particle transport. Each sawtooth gives an additional diffusion coefficient of the order of r_{ST}^2/t_{ST} ($=0.5$ m^2/s) [21], which is not included in our analysis. Sawtooth oscillations with inversion radius of $a/3$ exist in both the co-NBI and ctr-NBI phases. The period of the sawteeth is 10 ms in co-NBI and increases up to 20 ms in the early ctr-NBI phase and the sawteeth disappear 100–150 ms after the start of ctr-

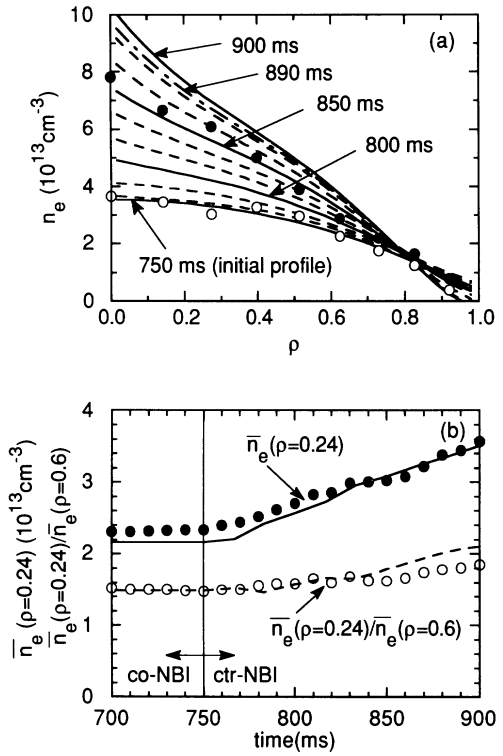

FIG. 3. Time evolution of (a) radial profile and (b) line-averaged electron density in ctr-NBI phase. In (a), lines are simulated profiles every 16.6 ms and open and solid circles are profiles in the co-NBI phase (t =690 ms) and in the ctr-NBI phase (t =890 ms) measured in TS. In (b), lines are simulated and open and solid circles are measured with FIR.

NBI. Since these sawteeth tend to make the electron density flat at $r < a/3$, the density peaking simulated here is overestimated due to the lack of the sawtooth effect in the model.

Finally we discuss the measurement errors. Since the toroidal rotation velocity becomes smaller and the poloidal rotation velocity becomes larger toward the plasma edge, the error in E_r due to the lack of measurements of the poloidal rotation is largest at the plasma edge. The edge radial electric field obtained from simultaneous toroidal and poloidal rotation measurements is typically ~ -50 V/cm for an L-mode plasma [22], which is consistent with the E_r obtained by using Eq. (1) within the accuracy of 20–30 V/cm. The uncertainty of E_r on the simulation is sufficiently small for the ctr-NBI phase.

In conclusion, peaking of the density profile is observed 30–80 ms after the neutral-beam direction is switched from coinjection to counterinjection. The inward pinch flux to produce this peaked electron density shows quantitative agreement with the inward pinch model.

The authors are greatly indebted to Dr. K. McCormick (Max-Planck-Institut für Plasmaphysik) for his helpful discussions. The authors thank Dr. K. Tani (Japan Atomic Energy Research Institute, JAERI) for making available the numerical codes of neutral-beam deposition power. We also thank Dr. H. Sanuki (National Institute for Fusion Science, NIFS) for discussion, and Dr. H. Maeda (JAERI) and Dr. T. Hamada (NIFS) for their continuous encouragement.

[1] M. Greenwald *et al.*, Phys. Rev. Lett. **53**, 352 (1984).
[2] J. D. Strachan *et al.*, Phys. Rev. Lett. **58**, 1004 (1987).
[3] F. X. Soldner *et al.*, Phys. Rev. Lett. **61**, 1105 (1988).
[4] K. McCormick *et al.*, J. Nucl. Mater. **176&177**, 89 (1990).
[5] M. Mori *et al.*, Nucl. Fusion **28**, 1891 (1988).
[6] O. Gehre *et al.*, Phys. Rev. Lett. **60**, 1502 (1988).
[7] V. Mertens *et al.*, Plasma Phys. Controlled Fusion **32**, 965 (1990).
[8] S. Scott *et al.*, Phys. Rev. Lett. **64**, 531 (1990).
[9] J. A. Snipes *et al.*, Nucl. Fusion **30**, 205 (1990).
[10] M. Murakami *et al.*, in *Proceedings of the Tenth International Conference on Plasma Physics and Controlled Nuclear Fusion Research, London, 1984* (IAEA, Vienna, 1985), Vol. I, p. 87.
[11] K. C. Shaing, Phys. Fluids **31**, 2249 (1988).
[12] S.-I. Itoh, J. Phys. Soc. Jpn. **59**, 3431 (1990).
[13] G. A. Hallock, J. Mathew, W. C. Jennings, and R. L. Hickok, Phys. Rev. Lett. **56**, 1248 (1986).
[14] K. Ida and S. Hidekuma, Rev. Sci. Instrum. **60**, 867 (1989).
[15] F. L. Hinton and R. D. Hazeltine, Rev. Mod. Phys. **48**, 239 (1976).
[16] B. Coppi and C. Spight, Phys. Rev. Lett. **41**, 551 (1978).
[17] F. Romanelli, Phys. Fluids B **1**, 1018 (1989).
[18] R. D. Hazeltine, S. M. Mahajan, and D. A. Hichcock, Phys. Fluids **24**, 1164 (1981).
[19] D. Pasini *et al.*, Nucl. Fusion **30**, 2049 (1990).
[20] R. Giannella *et al.*, in *Proceedings of the Eighteenth European Conference on Controlled Fusion and Plasma Heating, Berlin, 1991* (European Physical Society, Petit-Lancy, 1991), Vol. 15C, Pt. I, p. 197.
[21] K. Ida, R. J. Fonck, R. A. Hulse, and B. Leblanc, Plasma Phys. Controlled Fusion **28**, 879 (1986).
[22] K. Ida, S. Hidekuma, Y. Miura, T. Fujita, M. Mori, K. Hoshino, N. Suzuki, T. Yamauchi, and JFT-2M Group, Phys. Rev. Lett. **65**, 1364 (1990).